MHD waves in small magnetic elements: comparing IMaX observations to simulations

M. Stangalini[1], S. K. Solanki[1,2], and R. Cameron[1]

[1] Max Planck Institute for Solar System Research, Max-Planck-Str. 2 37191 Katlenburg-Lindau Germany, e-mail: `stangalini@mps.mpg.de`
[2] School of Space Research, Kyung Hee University, Yongin, Gyeonggi 446-701, Republic of Korea

Abstract. Small-scale magnetic fields are thought to play an important role in the heating of the outer solar atmosphere. By exploiting the high-spatial and temporal resolution of IMaX, the bidimensional spectropolarimeter on board the Sunrise balloon-borne observatory, we study the excitation of MHD waves in small magnetic elements, providing clues on the interaction of the magnetic structures with the photospheric forcing and the ambient acoustic field. The large fraction of magnetic features observed by IMaX made it possible to study the interaction between the photospheric granulation and the flux tubes from a statistical point-of-view. In particular we find a 90 degree phase lag with an high confidence level between the horizontal displacements of the flux tubes and the velocity perturbations measured inside them. We also find that the observational results are in excellent agreement with MHD simulations. This result suggests that the horizontal displacement of small-scale magnetic features by the surrounding granulation excites longitudinal waves within the magnetic elements.

Key words. Sun: photosphere – Sun: oscillations

1. Introduction

Magnetic fields are ubiquitous in the solar atmosphere and manifest over a wide range of spatial scales, from big sunspots with diameters of the order of 70000 Mm, down to small elements at or below the current spatial resolution achieved by modern solar telescopes ($\sim$ 100 km, see for example Solanki et al. 1999; Lagg et al. 2010; Bonet et al. 2012).

Interestingly, magnetic fields can guide MHD waves through different layers in the solar atmosphere, thus contributing actively to the energy budget and the dynamics of the atmosphere itself (Narain & Ulmschneider 1996; De Pontieu et al. 2004). Small magnetic elements can support a large variety of modes of oscillations (Edwin & Roberts 1983; Roberts 1983; Khomenko et al. 2008; Erdélyi & Fedun 2010; Fedun et al. 2011, to name a few). From the observational point-of-view, only few observational studies of waves in small magnetic elements exist (Volkmer et al. 1995; Martínez González et al. 2011; Jess et al. 2012b,a). In particular, Jess et al. (2012b) found upward propagating longitudinal waves in small magnetic elements as periodic intensity fluctuations in the range $110 - 600$ s.

Send offprint requests to: M. Stangalini

(a) IMaX longitudinal field

(b) B_z MHD simulation
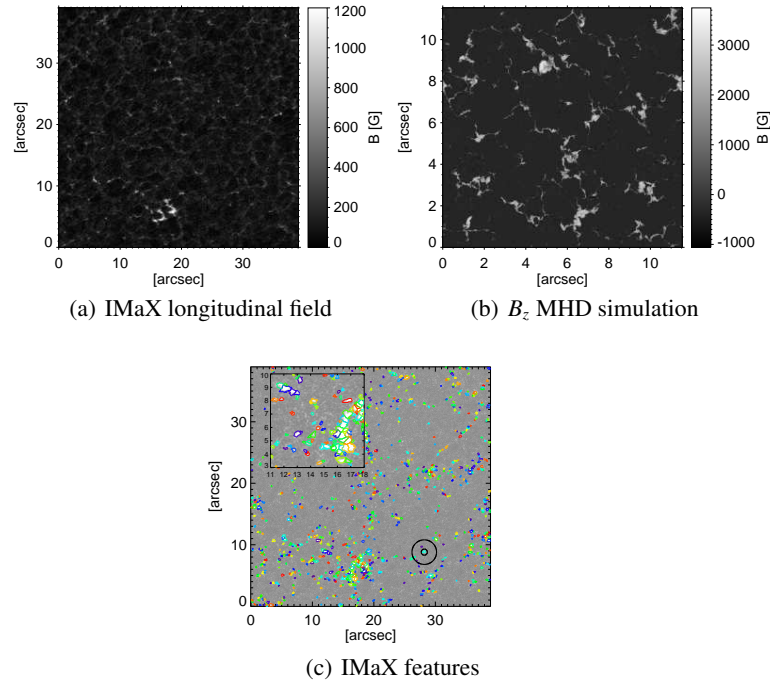

(c) IMaX features

Fig. 1. (a) IMaX longitudinal field obtained from SIR inversions. (b) MHD simulation: longitudinal component of the magnetic field. (c) IMaX features tracking example. The two concentric circles bound the region surrounding the magnetic feature in which we consider the p-mode oscillations. Each color represents a label.

Hasan et al. (2003) argued that horizontal motion of magnetic elements in the photosphere can generate enough wave energy to heat the magnetized chromosphere. They found that granular buffeting excites kink waves and, through non-linear mode coupling, longitudinal waves. Musielak & Ulmschneider (2003) demonstrated in fact that, although transverse tube waves do not generate observable Doppler signals, they excite forced and free longitudinal oscillations, detectable in Doppler shifts, through non-linear coupling.

In this contribution, we take advantage of the unprecedented combination of high spatial and high temporal cadence provided by SUNRISE/IMaX to study the interaction between kink oscillations and longitudinal oscillations in small magnetic elements in the solar photosphere. Our observational results are also compared with MHD simulations.

2. SUNRISE/IMaX Observations and the MHD simulation

The data set used in this work consists of a 2D spectropolarimetric time series acquired by the Imaging Magnetograph eXperiment (IMaX; Martínez Pillet et al. 2011) on board the SUNRISE balloon-borne mission (Barthol et al. 2010) in the Fe I 525.02 nm spectral line. The data were taken on 2009 June 9 and encompass a quiet Sun region of approximately 40×40 arcsec close to disk center. The total duration and the temporal cadence are respectively 32 min and 33 s. The data were phase-diversity reconstructed (Solanki et al. 2010; Martínez Pillet et al. 2011), and the spatial resolution is $0.15 - 0.18$ arcsec. For further information on the calibration procedure of IMaX data we refer to Roth et al. (2010).

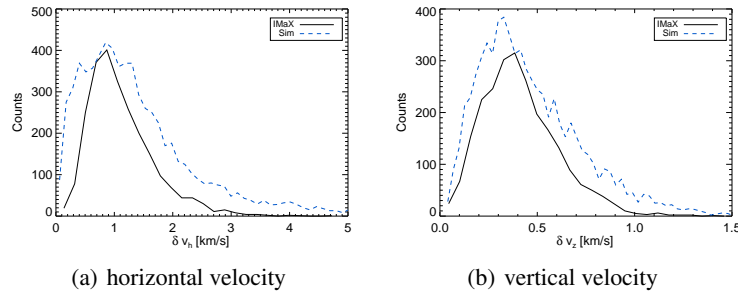(a) horizontal velocity   (b) vertical velocity

Fig. 2. (a) Histogram of amplitudes of the horizontal velocity. (b) Histogram of amplitudes of the vertical velocity.

In Fig. 1 we show the longitudinal magnetic field (panel a) estimated by means of SIR spectropolarimetric inversions (Ruiz Cobo & del Toro Iniesta 1992), assuming a single-component atmosphere with height-independent magnetic vector.

The MHD simulation used in this work was obtained through the MURaM code (Vögler et al. 2005). The simulation box is $20 \times 24 \times 2.3$ Mm (see Fig. 1 b) although we only considered the layer $\tau = 1$ in our analysis. The grid spacing is 20.8 km in both horizontal directions, and 14 km in the vertical. The top boundary is open to flows, and the magnetic field there is forced to be vertical.

3. Methods

In this work we study the longitudinal and kink waves in small magnetic elements. To this aim we track the magnetic features using the YAFTA code (Yet Another Feature Tracking Algorithm; Welsch & Longcope 2003). The algorithm tracks and labels groups of pixels lying on the same 'hill' in unsigned circular polarization maps, in the case of IMaX data, and vertical magnetic field maps in the case of simulations. We set up two thresholds. The first detection threshold is set at 2σ, this means that every pixel below this limit is not considered. The second threshold acts spatially allowing the detection of only those magnetic features whose area is larger than 9 pixels (slightly larger than the spatial resolution achieved) in the case of IMaX data, and 49 pixels for the

MHD simulation. In Fig. 1 (panel c) we give an example of features fulfilling the criteria in a SUNRISE/IMaX snapshot. Each color represents a label for the identification of the magnetic elements.

Since we are mainly interested in the analysis of the spectrum of oscillations, all the features lasting for less than 150 s are rejected. This is done to increase the frequency resolution in our analysis.

Our primary aim is to study the interaction between kink oscillations and longitudinal oscillations by exploiting the large number of features observed. The total number of features tracked in the IMaX data and the simulation amounts to 2384 and 6388, respectively.

For each magnetic element tracked by the algorithm, we estimate the vertical velocity (v_z) within its area (LoS velocity in the case of IMaX data, since the FoV is close to disk center), and the horizontal velocity (v_h) obtained by following its position. Note that we only consider one component of the horizontal velocity in this case (i.e. v_y). We refer to it simply as the horizontal velocity. The Doppler velocity and the magnetic field are estimated through SIR spectropolarimetric inversions.

In addition we also estimate the contribution of the ambient photospheric oscillatory field (v_{ac}) by considering a surrounding region like that shown in Fig. 1 (lower right part of panel c). The two radii specifying the aperture are respectively about 380 km and 950 km. The acoustic field signal is estimated by taking the average of the velocity of the non-magnetic
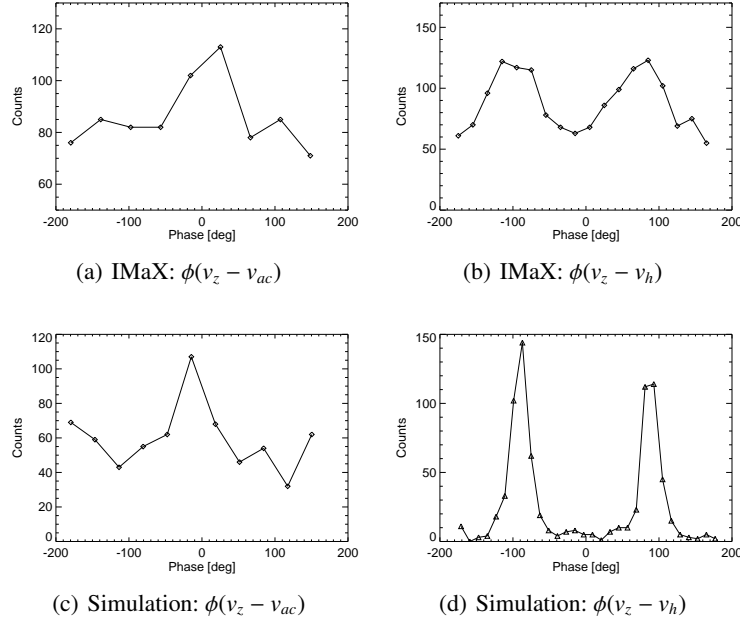
(a) IMaX: $\phi(v_z - v_{ac})$

(b) IMaX: $\phi(v_z - v_h)$

(c) Simulation: $\phi(v_z - v_{ac})$

(d) Simulation: $\phi(v_z - v_h)$

Fig. 3. (a) Histogram of phase $\phi(v_z - v_{ac})$ obtained from IMaX between the vertical velocity v_z in magnetic features and p-mode velocity in surroundings, v_{ac}.(b) Histogram of phase $\phi(v_z - v_h)$ from IMaX, where v_h is the horizontal velocity of magnetic features. (c) Histogram of phase $\phi(v_z - v_{ac})$ from MHD simulations. (d) Histogram of phase $\phi(v_z - v_h)$ from MHD simulations. Only those signals with a coherence larger than 0.8 outside the cone-of-influence of the wavelet diagram contribute to a histogram.

pixels (below 10 G) within the defined aperture. This prevents contamination by possible magnetic field effects.

To study the relation between the different velocity perturbations, we employ a phase lag analysis on both simulations and observations. This analysis is performed by using the wavelet code by Torrence & Webster (1999).

In the coherence diagram, given by the wavelet, we consider only those points for which the coherence is above 0.8 outside the cone-of-influence, i.e. in the region where the wavelet analysis can be trusted. This high threshold ensures the interaction between the two modes under investigation. In this case we compute the phase lag $\phi(v_z - v_{ac})$, and $\phi(v_z - v_h)$. We repeat this analysis for each magnetic element tracked, obtaining the histograms of the phase.

4. Results

From the feature tracking we obtain the horizontal and vertical velocity associated to each magnetic element. To characterize the oscillations present in the magnetic elements, in Fig. 2 we show the distributions of the standard deviation of these two quantities for both simulations and observations. Most of the magnetic elements have a horizontal amplitude of oscillation around 1 km/s, while the longitudinal velocity amplitude is $\sim 0.3 - 0.4$ km/s.

In Fig. 3 we plot the results of the phase analysis obtained from IMaX observations (upper panels) to those from the MHD simulation (bottom panels). The left panels represent the phase histogram between the vertical velocity within the magnetic features and the acoustic signal, the right panels the phase between the vertical velocity and the horizontal one. The phase histograms obtained from

the MHD simulation display peaks at the same phases as the IMaX data.

The phase histogram $\phi(v_z - v_{ac})$ shows a considerable maximum at $0°$. Thus the vertical velocity inside the magnetic structures is in phase with the surrounding Doppler velocity signal. Of greater interest are phase histograms $\phi(v_z - v_y)$. Both the IMaX data and the simulation display clear maxima at $-90°$ and $+90°$. It is worth stressing that the phase is estimated in the positions of the wavelet diagram where a high coherence is found. This selects only those components of the signals for which the interaction is strong.

To test the consistency of these results and, in particular, the $\pm90°$ phase lag between the horizontal velocity and the vertical velocity inside the magnetic elements, we estimate the phase relation between the horizontal velocity and the longitudinal velocity surrounding the magnetic features, within an area of 800 km from the magnetic element, to check whether the $\pm90°$ phase lag is inherent the velocity field inside the flux tubes or it is due to some issue concerning the analysis. The results of this check are plotted in Fig. 4. The phase lag is zero in this case, and this demonstrates that the $\pm90°$ phase lag between the vertical and horizontal velocities is only obtained if the internal velocity field of the flux tube is considered.

5. Discussion and conclusions

The results shown in this work demonstrate the interaction between transverse and compressive modes in small magnetic elements in the solar photosphere. These interactions are illustrated by the phase relations shown in Fig. 3.

The velocity signal inside small magnetic elements is the result of the superposition of many components. Some of them are in relation with the surrounding oscillatory field, others with the horizontal velocity of the structures themselves.

While the surrounding oscillatory field outside the magnetic elements is in phase with the internal perturbations relevant to it, the horizontal velocity is found to be $90°$ out-of-phase with the vertical velocity.
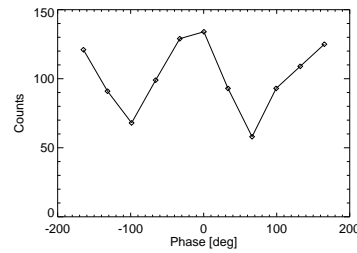

Fig. 4. Histogram of phase $\phi(v_h - v_{ac})$ obtained from IMaX data.

Unfortunately, the phase shift alone is not enough to uniquely identify the mode of oscillation. This is because, the vertical velocity in both the observations and the realistic MHD simulations used in this work, is possibly the result of a mixture of modes, whose superposition hinders their identification.

However, we argue that both the surrounding oscillatory field and the horizontal oscillations of the flux tube interact with the internal longitudinal velocity, and these interactions are characterized by fixed phase relations. More in detail, the kink oscillations are also accompanied by compressional modes responsible for the longitudinal perturbations of the velocity. Our results are based upon statistics and derived for a large number of magnetic elements for which the internal velocity field is resolved thanks to the high spatial resolution provided by SUNRISE/IMaX.

The presence of detectable LoS velocity oscillations inside the flux tubes, associated with horizontal displacements, is in agreement with the theoretical work by Hasan et al. (2003) and Musielak & Ulmschneider (2003). These authors argued that the horizontal displacement of the flux tubes, due to the external forcing by granular buffeting, not only generates kink oscillations, but also longitudinal oscillations, which should then be observable inside the magnetic structures as Doppler velocity oscillations. Our results are consistent with this scenario.

Moreover, Nakariakov & Verwichte (2005) have also shown, by means of numerical simulations, that longitudinal compressive waves are excited by the kink mode (see their Fig.

4 and the online movie[1]). Their simulation demonstrates that the longitudinal perturbation is 90° out of phase with respect to the kink mode. More in detail, the longitudinal mode reaches its maximum when the flux tube inverts its trajectory (i.e. when $v_h = 0$). Our results are also consistent with the above scenario, although this is possibly not the only reason for the 90° phase lag between the horizontal and vertical velocity. To this regard, a detailed analysis of a few isolated cases in the MHD simulation may help to investigate the process of interaction of different modes in small flux tubes and to identify their nature.

References

Barthol, P., et al. 2010, Sol. Phys., 268, 1

Bonet, J. A., Cabello, I., & Sánchez Almeida, J. 2012, A&A, 539, A6

De Pontieu, B., Erdélyi, R., & James, S. P. 2004, Nature, 430, 536

Edwin, P., & Roberts, B. 1983, Sol. Phys., 88, 179

Erdélyi, R., & Fedun, V. 2010, Sol. Phys., 263, 63

Fedun, V., Shelyag, S., & Erdélyi, R. 2011, ApJ, 727, 17

Hasan, S. S., Kalkofen, W., van Ballegooijen, A. A., & Ulmschneider, P. 2003, ApJ, 585, 1138

Jess, D. B., et al. 2012a, ApJl, 744, L5

Jess, D. B., et al. 2012b, ApJ, 746, 183

Khomenko, E., Collados, M., & Felipe, T. 2008, Sol. Phys., 251, 589

Lagg, A., et al. 2010, ApJl, 723, L164

Martínez González, M. J., et al. 2011, ApJ, 730, L37

Martínez Pillet, V., et al. 2011, Sol. Phys., 268, 57

Musielak, Z. E., & Ulmschneider, P. 2003, A&A, 406, 725

Nakariakov, V. M., & Verwichte, E. 2005, Living Reviews in Solar Physics, 2

Narain, U., & Ulmschneider, P. 1996, Space Sci. Rev., 75, 453

Roberts, B. 1983, Sol. Phys., 87, 77

Roth, M., et al. 2010, ApJl, 723, L175

Ruiz Cobo, B., & del Toro Iniesta, J. C. 1992, ApJ, 398, 375

Solanki, S. K., et al. 2010, ApJl, 723, L127

Solanki, S. K., Finsterle, W., Rüedi, I., & Livingston, W. 1999, A&A, 347, L27

Torrence, C., & Webster, P. J. 1999, Journal of Climate, 12, 2679

Vögler, A., et al. 2005, A&A, 429, 335

Volkmer, R., Kneer, F., & Bendlin, C. 1995, A&A, 304, L1

Welsch, B. T., & Longcope, D. W. 2003, ApJ, 588, 620

---

[1] The movie of the simulation is available here: `http://solarphysics.livingreviews.org/Articles/lrsp-2005-3/resources/cylindermodes/fast_m1_b0_running/java_movieplayer_trans.html`